International Journal of Nanomedicine

Dovepress
open access to scientific and medical research

Open Access Full Text Article

ORIGINAL RESEARCH

Role of surface modification in zinc oxide nanoparticles and its toxicity assessment toward human dermal fibroblast cells

This article was published in the following Dove Press journal:
International Journal of Nanomedicine
7 August 2014
Number of times this article has been viewed

Mohankandhasamy Ramasamy[1]
Minakshi Das[1]
Seong Soo A An[1]
Dong Kee Yi[2]

[1]Division of Bionanotechnology, Gachon University, Seongnam, [2]Department of Chemistry, Myongji University, Yongin, South Korea

Abstract: The wide-scale applications of zinc oxide (ZnO) nanoparticles (NPs) in photocatalysts, gas sensors, and cosmetics may cause toxicity to humans and environments. Therefore, the aim of the present study was to reduce the toxicity of ZnO NPs by coating them with a silica (SiO_2) layer, which could be used in human applications, such as cosmetic preparations. The sol–gel method was used to synthesize core ZnO with SiO_2-shelled NPs (SiO_2/ZnO NPs) with varying degrees of coating. Diverse studies were performed to analyze the toxicity of NPs against cells in a dose- and time-dependent manner. To ensure the decreased toxicity of the produced SiO_2/ZnO NPs, cytotoxicity in membrane damage and/or intracellular reactive oxygen species (ROS) were assessed by employing 3-(4,5-dimethylthiazol-2-yl)-2,5-diphenyltetrazolium bromide, lactate dehydrogenase, 2′,7′-dichlorofluorescin, and lipid peroxide estimations. The cores of ZnO NPs exhibited cytotoxicity over time, regardless of shell thickness. Nevertheless, the thicker SiO_2/ZnO NPs revealed reduced enzyme leakage, decreased peroxide production, and less oxidative stress than their bare ZnO NPs or thinner SiO_2/ZnO NPs. Therefore, thicker SiO_2/ZnO NPs moderated the toxicity of ZnO NPs by restricting free radical formation and the release of zinc ions, and decreasing surface contact with cells.

Keywords: zinc oxide, silica coating, photostability, human dermal fibroblast, membrane damage, oxidative stress

Introduction

Advancements in science and technology have brought the promising tools of nanotechnologies for making diverse nanomaterials for various applications. In recent years, various studies have focused on diverse platforms to improve nanomaterial properties by altering the particle composition, size, and surface characterizations to make better and safer nanomaterials.[1–5] Among these, heterostructured inorganic nanoparticles (NPs) have become predominant materials for their high quantum confinement effects, and could be used in expanding solar cell and photocatalyst applications.[6–8] Furthermore, various core–shell NPs have exhibited unique properties for their respective applications in many fields of engineering and medicine.[9–15]

Due to its semiconductivity, high transparency, large surface-to-volume ratio, and better ultraviolet (UV)-ray absorption, nanometer-scaled ZnO is regarded as a highly applicable nanomaterial in the fields of optoelectronics, photonics, clothing, paint, sports accessories, medicine, and cosmetics.[16–21] Nowadays, ZnO NPs are being widely used as a UV protector in modern personal care products, such as sunscreen creams. On the other hand, an increased number of nanobased products could bring greater risks to humans, wherein nanomaterials could enter biological systems through

Correspondence: Seong Soo A An
Division of Bionanotechnology, Gachon University, 1342 Seongnamdaero, Sugeong-gu, Seongnam, Gyeonggi-do 461 701; South Korea
Tel +82 31 750 8981
Email seongaan@gc.gachon.ac.kr

Dong Kee Yi
Department of Chemistry, Myongji University, 116 Myongji-ro, Cheoin-gu, Yongin, Gyeonggi-do 449 728, South Korea
Tel +82 31 330 6178
Email vitalis@mju.ac.kr

different routes of exposure.[22,23] Although reports on the safety/toxicity of inorganic NPs on skin are on the rise, toxicological evidence is still limited, especially for ZnO NPs. Previous studies have reported that ZnO NPs produce high toxicities in various biological systems, such as in many cellular organisms from bacteria, to fish, to mice.[24–30] A possible reason for this observed toxicity is reactive oxygen species (ROS) produced from the meta-based nanoparticles leading to oxidative stress. In addition, after stronger light absorption by the photocatalyst, free electrons and holes can be produced by NPs, leading to the production of free hydroxyl radicals by strong oxidation.[31–33]

Structurally, the surface chemistry of nanosized metal particles became a critical factor in designing cellular interactions with biological molecules in vitro.[34] Different toxicological responses can be obtained from unmodified core–shell and surface-modified NPs in various cell lines.[35–37] Insulating a toxic core with a nontoxic shell improves solubility, enhancing ease of functionalization with reduced toxicity.[35,38] These results suggest that the toxic effects of NPs can be controlled through surface modifications.

Several publications have reported the toxicity of ZnO NPs in different organisms and cells. In order to overcome the toxicity, several studies have focused on the fundamental mechanisms of ZnO toxicity by designing novel approaches in producing biocompatible ZnO NPs. In this study, we developed controlled ZnO NPs with silica shells at different thicknesses without altering their desired physical properties, and their cytotoxicity was compared against bare ZnO NPs in vitro. Human skin dermal fibroblast neonatal (HDFn) cells were used as a cell model to assess potential toxicity, since dermal fibroblasts could be the first portal of entry to many toxicants from the outer environment.[39] Various cytotoxicity parameters, such as cell-morphology analysis, cellular uptake, 3-(4,5-dimethylthiazol-2-yl)-2,5-diphenyltetrazolium bromide (MTT), lactate dehydrogenase (LDH), lipid peroxide (LPO), and intracellular ROS assays, were employed.

Materials and methods

Materials

ZnO suspension (30 wt% in ethanol; Advanced Products, Daejeon, South Korea), tetraethyl orthosilicate (TEOS; 99.999%; Sigma-Aldrich, St Louis, MO, USA), ethanol (99.9%; Samchun Chemical, Seoul, South Korea), and ammonium hydroxide (NH_4OH 25%–28%; Sigma-Aldrich, St Louis, MO, USA) were purchased. In-house Milli-Q® water (EMD Millipore, Billerica, MA, USA) was used throughout the experiments.

Synthesis of silica-coated zinc oxide nanoparticles

NP hybrids were synthesized using a modified sol-gel process, as reported previously.[40] In brief, ethanol (35 mL), water (15 mL), and NH_4OH (10 mL, pH 12) were poured into a round-bottomed flask (100 mL) with stirring at room temperature. ZnO (0.5 g) was dispersed with TEOS (30 and 80 wt% to the respective amount of ZnO) and injected into the reaction flask. After ultrasonic treatment for 10 minutes, the colloidal dispersion was stirred overnight for the complete hydrolysis of TEOS.[41] NPs were collected by centrifugation at 5,000 rpm (2-16PK; Sigma-Aldrich), washed subsequently with ethanol three times, and then dried overnight in a vacuum oven at 60°C. The thin and thick silica coating was achieved by adjusting the TEOS to the ZnO weight ratio. Pure ZnO NPs were labeled as bare ZnO NPs, and silica-coated NPs were labeled as thin or thick SiO_2/ZnO NPs.

Characterizations

The morphologies of NPs were characterized using high-resolution transmission electron microscopy (HR-TEM; Tecnai™ G2 TF 30ST; FEI, Hillsboro, OR, USA). The silica-shell thickness in each particle was measured; at least three particles were measured per image. Elemental analysis of the identical NPs was performed using energy-dispersive X-ray spectroscopy (EDX) interfaced with HR-TEM. Hydrodynamic diameters and the zeta potentials were measured using dynamic light scattering with a Malvern Zetasizer 3000HS (Malvern Instruments, Malvern, UK) for the particle-size distribution and electrokinetic behavior of the NPs at pH 7. The degree of photodegradation was assessed by measuring the photoluminescence (PL) using a spectrofluorometer (Varian Cary Eclipse; Agilent Technologies, Santa Clara, CA, USA). Bare ZnO and thin and thick SiO_2/ZnO NPs were exposed to UV light (CN-6 UV lamp, 60 HZ with 365 nm) for a maximum of 72 hours, and the respective PL-intensity responses were recorded at intervals of 4 hours.

Cell culture and exposure to NPs

HDFn cells from the Korea Cell Line Bank (Seoul, South Korea) were cultured in supplemented Dulbecco's Modified Eagle's Medium with 10% fetal bovine serum and 1% penicillin, streptomycin, and amphotericin mixture at 37°C in a humidified atmosphere of 5% CO_2. Confluence cells (85%) were subcultured in six-well plates or 96-well plates for 24 hours prior to the treatment. NPs were suspended in cell-culture medium to attain desired concentrations, and

were sonicated before administering them to the cells. Cells without NPs served as controls in each experiment.

Cellular uptake

Fluorescence laser-scanning microscopy (FLSM; Eclipse TE2000-U; Nikon, Tokyo, Japan) was employed to assess the cellular uptake of NPs. Previously, fluorescein isothiocyanate (FITC)-adsorbed SiO_2/ZnO NPs were synthesized, as previously reported.[42] Briefly, both thin and thick SiO_2 ZnO NPs was stirred for 48 hours in the dark at room temperature to attain FITC-SiO_2/ZnO NPs.

Cells cultured for 24 hours were added to the FITC-SiO_2/ZnO NPs at a concentration of 50 μg/mL. After 4 hours' incubation, cells were washed twice with phosphate-buffered saline (PBS) in order to remove excess NPs, and stained with 4′,6-diamidino-2-phenylindole dihydrochloride (DAPI). Cells were viewed under inverted-phase FLSM.

In addition, the endocytosis of NPs in cells was observed for 4 hours with field-emission scanning electron microscopy (FE-SEM; JSM-7500F; JEOL, Tokyo, Japan). Prior to imaging, the cells were fixed on the glass substrate by using an osmium tetroxide-based standard-fixation method. Then, they were sputter-coated before being analyzed under a microscope.

Cell morphology

For the morphological study, cells were incubated with uncoated and coated NPs at 50 μg/mL concentrations. After 48 hours of incubation, cellular morphological changes were assessed by using a Nikon phase-contrast microscope with attached digital camera (Diaphot 300).

Cell-viability assay

The cells were exposed to 0, 5, 10, 20, 30, 40, and 50 μg/mL suspensions of the NPs for 12, 24, and 48 hours. MTT (Sigma-Aldrich)/Dulbecco's Modified Eagle's Medium was added to each well and incubated for 3 hours. The MTT solution was aspirated, and dimethyl sulfoxide was added. The absorbance from the formed purple MTT formazan crystals was measured at 570 nm by using a microplate reader (VersaMax™; Molecular Devices, Sunnyvale, CA, USA).

LDH-leakage assay

The cytoplasmic enzyme LDH released into the cell-culture medium has been reported as an important toxicity indicator in vitro.[43] This assay was based on the nicotinamide adenine dinucleotide $(NAD)^+$ reduction by the LDH enzyme. For evaluating cytotoxicities of bare ZnO NPs and those with different shell thicknesses, cells were exposed to 0–50 μg/mL suspensions for 48 hours. The NP-exposed cell suspension was centrifuged at 300 *g* for 3 minutes. The supernatant was mixed with a TOX7 assay kit (Sigma-Aldrich) for enzymatic analysis. The stoichiometric conversion of tetrazolium dye by NAD^+ was detected at 490 nm (VersaMax).

Oxidative stress assay

Previous studies have suggested that oxidative stress and LPO play a major role in NP-elicited cell-membrane disruption, deoxyribonucleic acid (DNA) damage, and cell death.[44] Therefore, it is important to analyze oxidative stress markers for the produced ZnO NPs. At first, the production of intracellular ROS was estimated with the dichlorofluorescein (DCF) assay, measuring the conversion of H_2DCF (2′,7′-dichlorodihydrofluorescein) to fluorescent DCF by ROS.[45] Briefly, cultured cells were exposed to NP suspensions of 0–50 μg/mL for 48 hours, washed with PBS, and incubated with 20 μM H_2DCF-DA (2′,7′-dichlorodihydrofluorescein-diacetate; Thermo Fisher Scientific, Waltham, MA, USA) for 60 minutes at 37°C. After being washed, the produced fluorescence was then detected at excitation and emission wavelengths of 488 and 528 nm, respectively. The mean fluorescence intensity was analyzed using a spectrofluorometer (Victor 3; PerkinElmer, Waltham, MA, USA). Basal ROS generation in cells without NPs was used as control.

Lipid peroxide estimation

When NPs react with cellular macromolecules, malondialdehyde (MDA) is produced. MDA is a proven mutagen and carcinogenic compound that reacts with cellular components, leading to cell-cycle arrest and cell death.[26,46,47] Also, it is an important oxidative stress marker produced by lipid peroxidation. Therefore, LPO levels were estimated as previously reported.[48] Briefly, the cultured cells were exposed to different concentrations of NPs for 48 hours. Then, the cells were scraped off, washed with PBS, and homogenized using cell lysis buffer. Then, the mixture was centrifuged at 1,500 *g* for 10 minutes at 4°C. The ice-cooled supernatant of the cell extract was incubated with phosphate buffered saline (0.1 M) at 37°C for 60 minutes. Trichloroacetic acid was added to precipitate the cell contents, and the mixture was then centrifuged to remove the supernatant separately. Next, *tert*-butyl alcohol (1%) was added to the supernatant and boiled for 15 minutes. Finally, the absorbance of the mixture was recorded at 532 nm, and the formed malondialdehyde was measured.

Statistical analysis

All independent experiments were performed in triplicate for each experiment, and the results are expressed as means ± standard deviation. Statistically significant changes between samples and control were analyzed by one-way analysis of variance using InStat and Prism 3 (GraphPad Software, La Jolla, CA, USA). The results were considered statistically significant at $P<0.05$ for all tests.

Results and discussion

Particle characterizations

The HR-TEM images revealed that the hydrodynamic diameters of the nanoparticle suspensions were between 20 and 50 nm with sphere-like morphology (Figure 1A). From the drop-cast sample images, 200 random particles were measured, and their average sizes are given in Table 1. Also, dynamic light-scattering analysis revealed size distributions of dispersed particles of 76.8 nm for bare ZnO, 105.3 nm for thin SiO_2/ZnO, and 158.1 nm for thick SiO_2/ZnO NPs, which shows the uniform distribution of the particles. Also, the bare ZnO NPs showed a zeta-potential value of +33.0 mV. After modification, a charge reversal of –20.7 mV was obtained from the thin SiO_2/ZnO particles and –41.5 mV from the thick SiO_2/ZnO NPs. These loosely aggregated particles from the coating with SiO_2 showed a thin layer on the surface, with the finding that increasing the Si-to-Zn molar ratio increased covering-layer thickness from 2 to 7 nm. Upon close inspection, thinly coated ZnO NPs with SiO_2 showed an uncovered core in some areas of the particle (Figure 1B). However, the thickly coated particles revealed a homogeneous layer around each particle, with complete covering with an SiO_2 shell (Figure 1C). In the EDX spectra of the bare and SiO_2-coated samples (Figure 1, A'–C'), all characteristic peaks were well matched with their unique elements of Zn, O, and Si. The C and O peaks occurred due to the supporting substrate used for TEM sampling. And the increasing peak intensity of C and O along with Zn and Si occurred due to the elements present in the nanoparticles. Furthermore, quantitative elemental analyses of the bare ZnO particles were compared with those of the surface-modified particles, listed in Table 2. A 0.68 wt% of silica was observed from the thin SiO_2/ZnO NPs, whereas the thick SiO_2/ZnO NPs indicated 3.34 wt%.

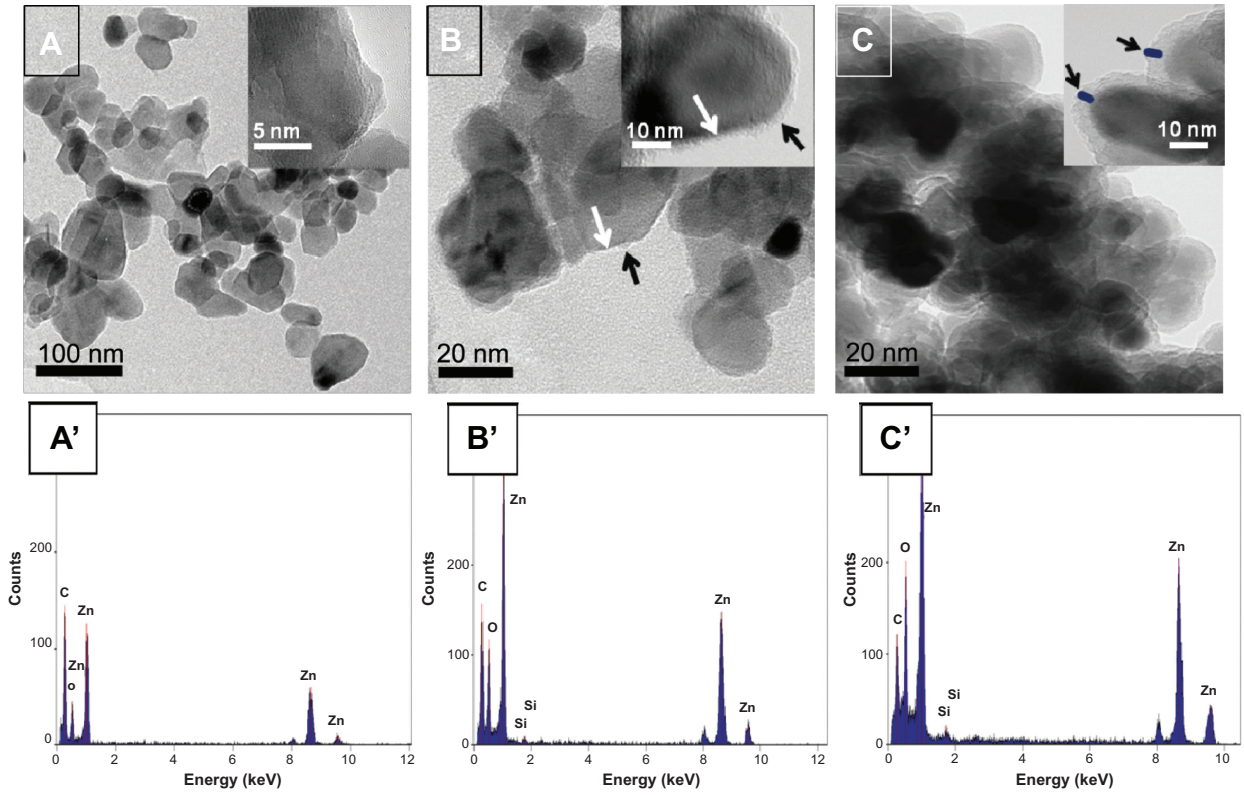

Figure 1 Characterization of ZnO NPs.

Notes: TEM images of (**A**) bare ZnO NPs, (**B**) thin SiO_2/ZnO NPs noted with black arrows of incomplete SiO_2 layer and ZnO core with white arrows, and (**C**) thick SiO_2/ZnO NPs (black arrows indicating the silica shell and its thicknesses), and their corresponding elemental spectrums, as shown in (**A'–C'**).

Abbreviations: ZnO NPs, zinc oxide nanoparticles; TEM, transmission electron microscopy; thin SiO_2/ZnO, ZnO coated with a thin layer of SiO_2; thick SiO_2/ZnO, ZnO densely coated with SiO_2.

Table 1 Characterization of coated and uncoated ZnO NPs

Parameters	Bare ZnO NPs	Thin SiO_2/ZnO NPs	Thick SiO_2/ZnO NPs
TEM (nm)	46.1±3	49.6±7.9	75.4±2.5
DLS in H_2O (nm)	76.8	105.3	158.1
PDI	0.12	0.19	0.21
Zeta-potential (mV)	+33.0	−20.7	−41.5

Abbreviations: ZnO NPs, zinc oxide nanoparticles; thin SiO_2/ZnO, ZnO coated with a thin layer of SiO_2; thick SiO_2/ZnO, ZnO densely coated with SiO; TEM, transmission electron microscopy; DLS, dynamic light scattering; H_2O, water; PDI, polydispersity index.

The increased Si contents were responsible for gaining silica thickness of 7 nm. The quantity of the Si peak was enhanced with increasing SiO_2 concentrations, which was in good agreement with the HR-TEM images. Meanwhile, higher SiO_2 concentrations decreased ZnO contents to 28.42 wt%, confirming the formation of dense silica shells on ZnO NPs. This was in good agreement with the elemental peaks presented in Figure 1.

The SiO_2/ZnO NPs were produced using a sol-gel method of TEOS through hydrolysis and subsequent condensation in the presence of NH_4OH to form a three-dimensional siloxane bond (Si–O–Si) by leaving an –OH group on the external surface. TEM images revealed darker cores surrounded by lighter shells, presumably due to the atomic number of Zn (65), which is higher than that of Si (28). The atomic weight-percentage quantification from EDX suggested the increased thickness of the silica shell, which made the particle surface distinct from the uncoated ZnO. A high negative zeta-potential value of the thick SiO_2/ZnO NPs was attributed to the bulky silica layer, with many Si–OH groups on the surface ensuring homogeneous dispersion. In addition, the cell viability of anionic thick SiO_2/ZnO NPs increased relatively in comparison with cationic bare ZnO NPs. This result was in agreement with previous reports, where cationic NPs strongly interacted with the negatively charged plasma membrane of the cell and thereby induced high toxicological responses.[49–51]

Figure 2 presents the PL response of the NPs after UV light (365 nm) exposure at different time intervals. For bare ZnO NPs, PL decreased significantly to 20% after 72 hours of incubation. In contrast, thick SiO_2/ZnO NPs ended with ~5% reduction. On the other hand, the thin SiO_2/ZnO NPs showed slow decreases of about 50% ZnO during the entire exposure time, which was slower than bare ZnO NPs but faster than thick SiO_2/ZnO NPs. From the photodegradation results, a thick SiO_2 shell over ZnO NPs either prevented the excited electrons from being involved in free radical formation or photoetching after monochromatic light exposure. Compared to the SiO_2/ZnO NPs, the bare ZnO NPs were attacked easily by the strong light due to photoetching, making them unstable.[52] This might have been due to the very thin silica shell or an incomplete silica layer, which was insufficient to prevent photocorrosion. Therefore, through high-energy irradiation like UV light, the photostability of ZnO was decreased due to increases in surface defects, occurring in the form of an energy gap, and thus the applied denser surface passivation decreased the interactions between external stimuli and core ZnO.

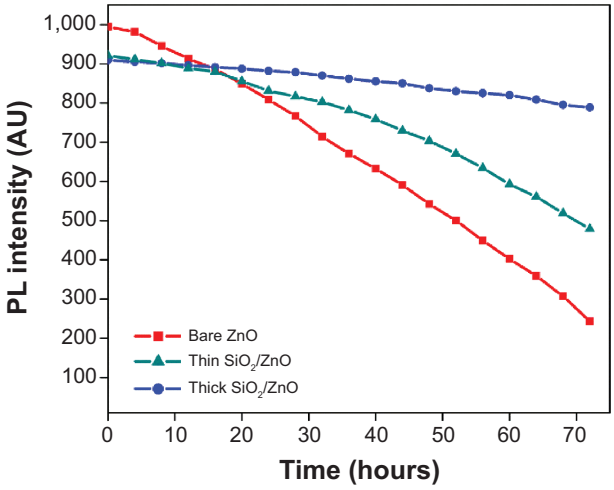

Figure 2 Photostability of ZnO NPs before and after surface modification.
Note: Change in the photoluminescence (PL)-intensity difference for the bare and functionalized NP suspensions under ultraviolet irradiation at different time intervals.
Abbreviations: ZnO NPs, zinc oxide nanoparticles; thin SiO_2/ZnO, ZnO coated with a thin layer of SiO_2; thick SiO_2/ZnO, ZnO densely coated with SiO.

Previously, we reported the photodegradation behavior of bare and silica-coated ZnO NPs against methylene blue solution.[53] We confirmed that after silica coating, the

Table 2 The percentage elemental composition of the coated and uncoated ZnO NPs from EDX analyses

Sample element	Bare ZnO NPs		Thin SiO_2/ZnO NPs		Thick SiO_2/ZnO NPs	
	Weight %	Atomic %	Weight %	Atomic %	Weight %	Atomic %
C (K)	40.75	66.19	41.81	65.56	46.91	67.42
O (K)	20.02	27.28	19.58	23.05	21.33	23.02
Si (K)	0	0	0.68	0.45	3.34	2.05
Zn (K)	39.23	6.53	37.93	10.93	28.42	7.51

Abbreviations: EDX, energy-dispersive X-ray spectroscopy; ZnO NPs, zinc oxide nanoparticles; thin SiO_2/ZnO, ZnO coated with a thin layer of SiO_2; thick SiO_2/ZnO, ZnO densely coated with SiO.

photodegradation ability of ZnO was reduced compared to the uncoated ZnO, which is in good agreement with previously reported results. This might have occurred because of the formed ROS on the ZnO surface after exposure to UV light.[54–56] Therefore, we are claiming that thick SiO_2/ZnO NPs could be used to make a better photostable agent with ZnO that maintains its desired physical properties the same as the bare ZnO NPs.

Cellular responses and cytotoxicity

To evaluate the cytotoxic potential of ZnO NPs, different cytotoxicity assays were performed for better reliability and reproducibility. Initially, the fate of NP suspensions in contact with HDFn cells was studied by FLSM (Figure 3). The images revealed that FITC-SiO_2/ZnO NP-exposed cells showed rapid cellular uptake within 4 hours. The uptake of NPs by fibroblasts appeared to be different for thin and thick SiO_2/ZnO NPs. Thin SiO_2/ZnO NP-incubated cells were monitored with discrete green fluorescence dots in the cytoplasm and nucleus by crossing the plasma membrane (marked by arrows). However, under the same experimental conditions, the thick SiO_2/ZnO NPs showed significantly higher internalization efficiency by the cell. NPs were internalized throughout the cells, except the nucleus, and appeared as bright multiple aggregates, potentially due to their accumulations inside each organelle, most likely through endocytosis. Like lysosomal colocalization of NPs in cytoplasm, multiple mechanisms of cellular uptake could be also possible.[57–59]

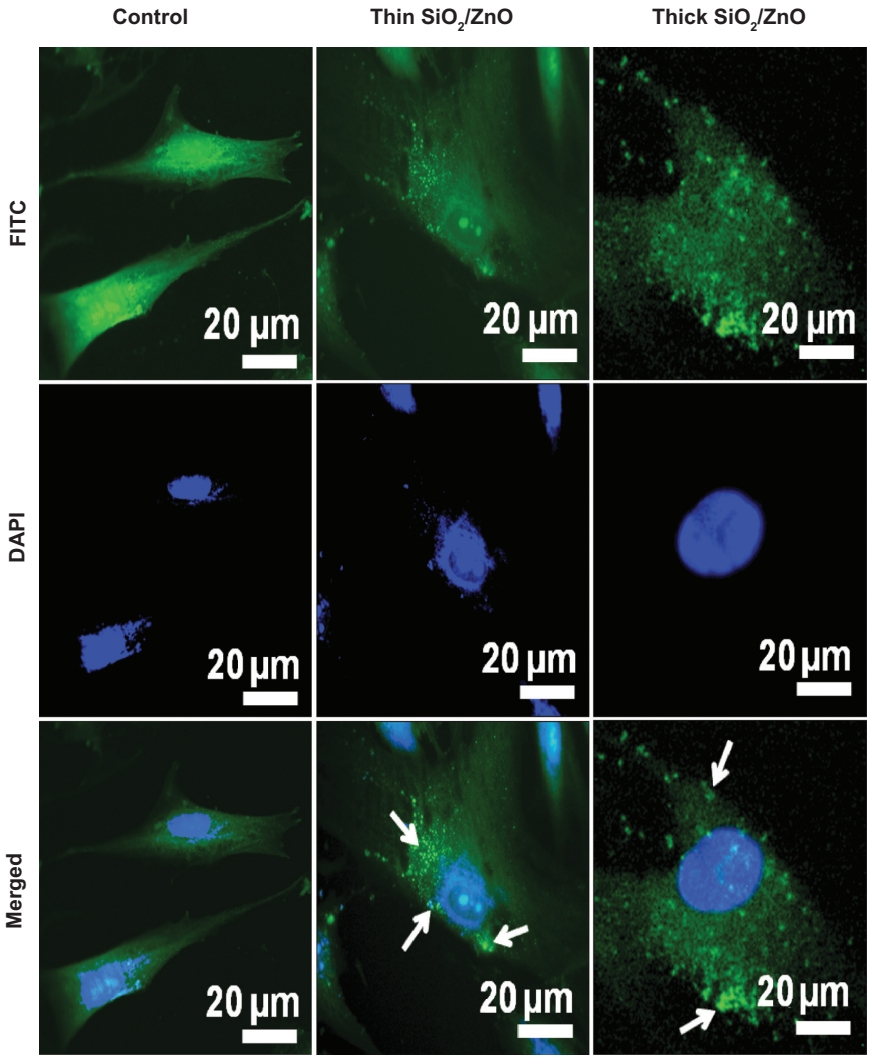

Figure 3 Association of NPs with cultured HDFn cells.
Notes: Fluorescence laser scanning microscopy of cellular internalization of FITC-loaded SiO_2/ZnO NPs (green). NP colocalization is indicated by arrows. The cell nucleus was stained with DAPI (blue). Scale bar 20 µm.
Abbreviations: NPs, nanoparticles; HDFn, human dermal fibroblast neonatal; FITC, fluorescein isothiocyanate; DAPI, 4′,6-diamidino-2-phenylindole dihydrochloride; thin SiO_2/ZnO, ZnO coated with a thin layer of SiO_2; thick SiO_2/ZnO, ZnO densely coated with SiO.

More accurate visualizations of the fate of NPs with regard to the cell was achieved using SEM imaging. There was a complete collapse of the cellular membrane after treatment with bare ZnO NPs, and the shape of grown cells became unorganized (Figure 4A). On the other hand, cellular exposure of thin SiO_2/ZnO NPs showed intact shapes of cells with a slight shrinking surface (Figure 4B). Lastly, incubated cells with the thick SiO_2/ZnO NPs did not reveal any cellular morphology or disturbance on the surface; instead, fully matured cells were observed (Figure 4C). Due to the higher atomic weight of ZnO, the bright-white dots were found on the cell components. In the focused view, the NP interactions with the cells were clearly observed. It was evident from the images (Figure 4, C and C') that the thick SiO_2/ZnO NPs caused minimal damage by maintaining a smooth and undisturbed

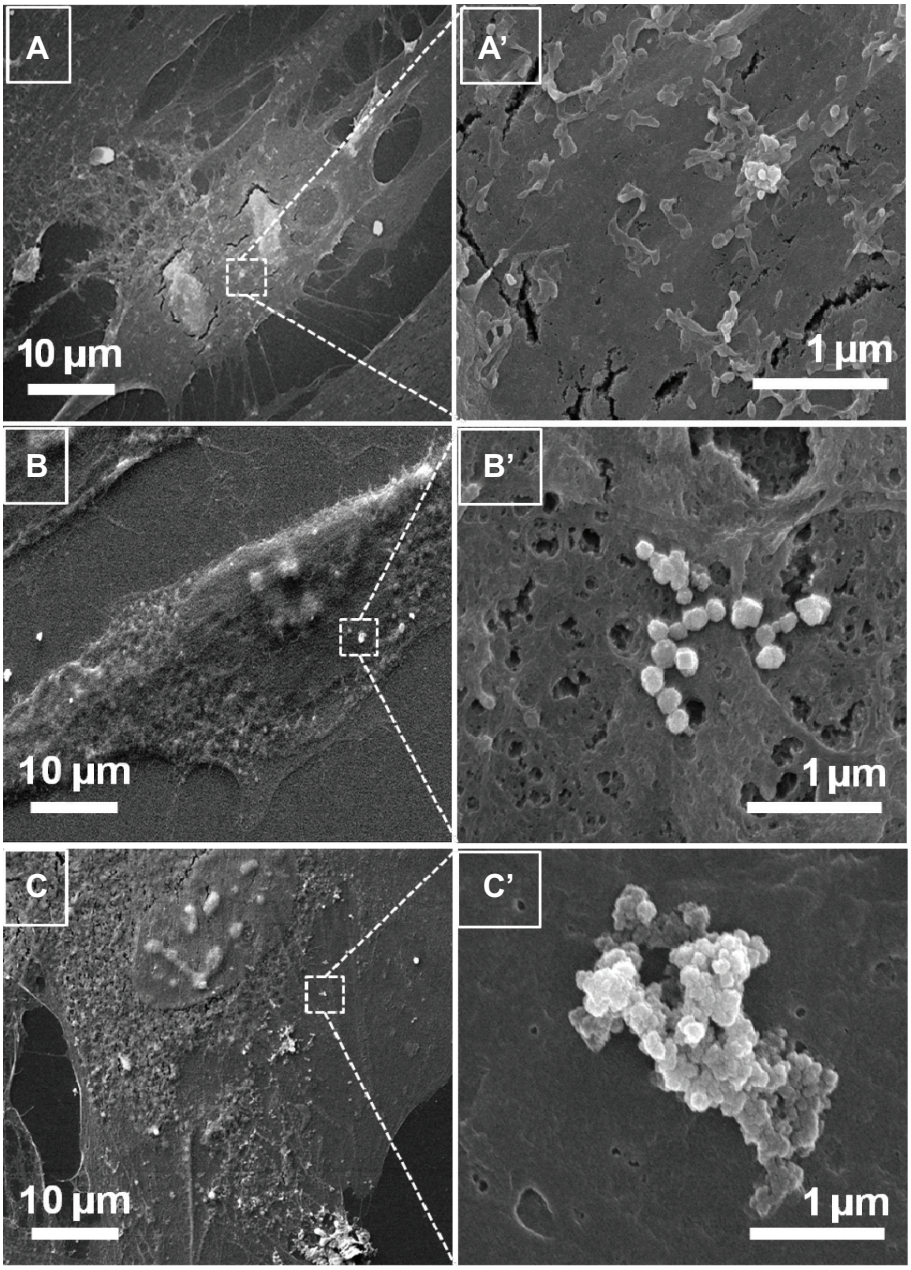

Figure 4 FE-SEM imaging for NP–cell interaction.
Notes: Cellular responses of HDFn cells after 4 hours' contact with (**A**) bare ZnO NPs, (**B**) thin SiO_2/ZnO NPs, and (**C**) thick SiO_2/ZnO NPs, and their corresponding enlarged views (**A'–C'**), respectively.
Abbreviations: FE-SEM, field-emission scanning electron microscope; HDFn, human dermal fibroblast neonatal; ZnO NPs, zinc oxide nanoparticles; thin SiO_2/ZnO, ZnO coated with a thin layer of SiO_2; thick SiO_2/ZnO, ZnO densely coated with SiO.

cell surface, whereas bare and thin SiO_2/ZnO NPs induced severe damage by deforming the cell components (Figure 4, A–B'). After being taken up by cells, both the uncoated and incompletely coated NPs entered into the nucleus and possibly denatured the nuclear proteins, since the regular cell cycle was damaged. In contrast, ZnO NPs densely covered with SiO_2 did not disturb the cell cycle and presumably did not enter into the nucleus, thus producing less cellular injury.[60] The biological fate of NPs in the cell components remains a controversial issue that needs clarification in future investigations.

Figure 5 shows the comparative responses of untreated and NP-treated HDFn cells. Cells exposed with bare ZnO NPs for 48 hours showed noticeable changes in morphology under microscopy. Compared to the elongated, matured, and undamaged control cells (Figure 5, A and A'), the ZnO NP-treated cells changed into spherical shapes and retracted from the surface, which resembled cell mortality (Figure 5, B and B'). The cells treated with thin SiO_2/ZnO NPs (Figure 5, C and C') showed similar shape changes to bare ZnO NP-treated cells. In contrast, cells treated with thick SiO_2/ZnO NPs (Figure 5, D and D') revealed more viable cells with fewer dead cells. The magnified view of single cells clearly indicated irrecoverable morphological damage, and thus injury occurred after treatment with NPs and led to cellular mortality.[61] The morphological changes are evidence of ZnO NP-induced toxicity in HDFn cells. Severe loss of normal morphology appeared in cells treated with bare and thin SiO_2/ZnO NPs, but not for thick SiO_2/ZnO NPs. A damaging tendency of NPs on the cell membrane was observed in magnified images. It is important to note that cellular viabilities were high in the presence of thickly coated NPs for long exposure times (48 hours) at 50 µg/mL relative to cells treated with uncoated NPs. These observations implied that the coatings on ZnO surface could be stable for longer periods.

Cell proliferation in response to various concentrations of bare, thin SiO_2, and thick SiO_2/ZnO NPs was also examined over time by MTT assays. At concentrations from 10 to 50 µg/mL, the viability of HDFn cells after exposure for 12, 24, and 48 hours to both the bare ZnO and thin SiO_2/ZnO NPs resulted in high mortality rates of about 97% and 95%, respectively (in 48 hours; A' and A'' as shown in Figure 6). In comparison, thick SiO_2/ZnO NPs exhibited lower toxicities, with cell viabilities of about 80% for 12 hours, 70% for 24 hours, and more than 50% for 48 hours (Figure 6A'''). The interpretation of cytotoxicity results can depend on the concentrations of NPs, which have been extensively discussed in the literature.[62–64] Exposure of uncoated

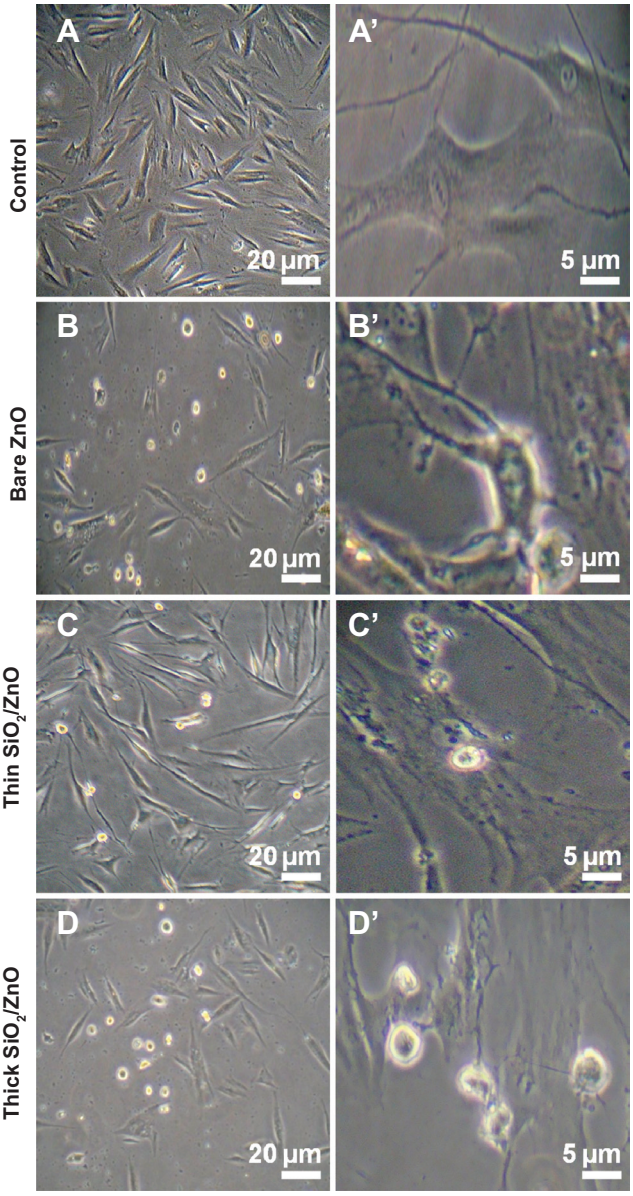

Figure 5 Morphology of HDFn cells exposed to NPs at 48 hours.
Notes: Normal (20 µm) and magnified views (5 µm) of (**A**, **A'**) control cells, (**B**, **B'**) bare ZnO NP-exposed cells, (**C**, **C'**) thin SiO_2/ZnO NP-exposed cells, and (**D**, **D'**) thick SiO_2/ZnO NP-exposed cells, respectively.
Abbreviations: HDFn, human dermal fibroblast neonatal; ZnO NPs, zinc oxide nanoparticles; thin SiO_2/ZnO, ZnO coated with a thin layer of SiO_2; thick SiO_2/ZnO, ZnO densely coated with SiO.

and thin SiO_2-coated ZnO NPs for 12, 24, and 48 hours resulted in a concentration-dependent increase in cell mortality and exhibited significant ($P<0.05$) cytotoxicity at 10–50 µg/mL concentrations, while thick SiO_2/ZnO NPs did not significantly decrease cell viability. The observed differences in cellular viability within the uncoated and thinly and thickly coated NPs suggested that the nature of the coating could also become a prominent factor under these conditions.

Previously, it has been demonstrated that a coating of SiO_2 on the surface of inorganic NPs with optimal

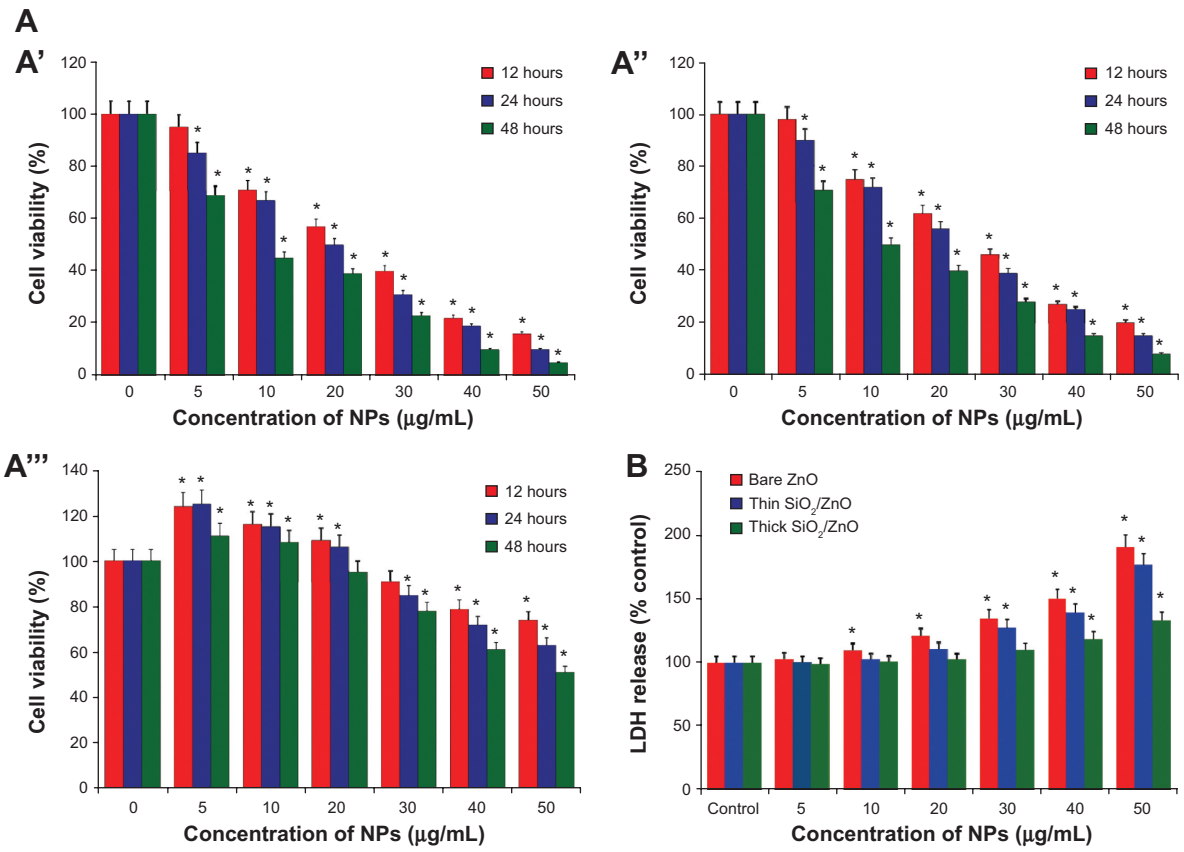

Figure 6 Cytotoxicity patterns of NPs to HDFn cells.
Notes: (**A**) Percentage cell viability of cells treated with (**A'**) bare ZnO NPs, (**A''**) thin SiO_2/ZnO NPs, and (**A'''**) thick SiO_2/ZnO NPs, and (**B**) LDH leakage of cells toward NPs at 48 hours. Control cells cultured in NP-free media were run in parallel to treatment groups. *$P<0.05$. Bars indicate standard deviation from individual triplicates.
Abbreviations: HDFn, human dermal fibroblast neonatal; ZnO NPs, zinc oxide nanoparticles; thin SiO_2/ZnO, ZnO coated with a thin layer of SiO_2; thick SiO_2/ZnO, ZnO densely coated with SiO; LDH, lactate dehydrogenase.

thicknesses could assist in reducing the cytotoxicity of the nanomaterials.[35,65] Also, it was explained that the release of zinc ion from ZnO NPs could harm the cell.

Here in our method, the bare ZnO NPs and thin SiO_2/ZnO NP-treated cells experienced severe cytotoxicity. This might have been because of the release of zinc ion from the NPs after reacting directly with the biological macromolecules present in the cell-culture medium. However, the thickly SiO_2-coated ZnO NPs showed lower cell mortality, which could have been due to less/no leaching of zinc ion from the NPs. Because the thick SiO_2 layer does not allow the cell to contact the ZnO core directly, this produced less toxicity. Also, the mesoporous structure in the SiO_2 layer maintained cell growth, as opposed to the hard ZnO core of the NPs, which damaged the cell membrane.[5,35,66,67]

With the observed differences between the uncoated and coated ZnO NPs, we can conclude that the nature of the surface coating influences decreases in the toxic effects of NPs.

To increase the reliability of the cytotoxicity data, the LDH-release assay was employed. Significantly increased LDH-release rates suggested a higher toxicity rate for the bare and thin SiO_2/ZnO NPs with increasing concentrations from 10 to 50 µg/mL ($P<0.05$) (Figure 6B). On the other hand, the degree of LDH leakage remained approximately 19% and 33% for 40 and 50 µg/mL of thick SiO_2/ZnO NPs, respectively, in comparison with the control group. Compared to controls, there was no significant induction in the LDH levels of HDFn cells treated with thick SiO_2/ZnO NPs. It is important to note that free LDH from incubated cells with surface-functionalized particles was significantly lower than their respective plain counterparts. A possible dissolution of zinc ions from ZnO NPs could be also considered as a cause of high cell mortality for the uncoated and unevenly thinly SiO_2-coated ZnO NPs.[24,68] The cytotoxicity of the bare and thinly SiO_2-coated ZnO NPs could presumably have mainly been related with the cellular damage of plasma membrane. Indeed, the physically incubated, uncoated, and incompletely coated NPs caused more damage to the cells, resulting in higher LDH leakage. Finally, it was evident from the results that the thick SiO_2 coating over ZnO NPs reduced the dissolution of zinc ion into the culture medium, thus maintaining

more viable cells. These results were significant, and correlated with those of Yin et al where reduced ZnO toxicity was observed after shielding of partial ZnO dissolution by surface coatings.[36]

The results in Figure 7A showed that ZnO NPs induced the generation of intracellular ROS in dose- and time-dependent manners, regardless of surface coating. In comparison to the control group (100%), the thick SiO_2/ZnO NPs produced 30% less ROS at 50 µg/mL, whereas bare and thin SiO_2/ZnO NPs at the same concentration induced higher levels of 97% and 80% ROS, respectively.

The ROS generated by ZnO NPs in HDFn cells induced lipid peroxidation, which could have been another factor in oxidative stress induction. Therefore, we analyzed LPO levels for 48 h. As shown in Figure 7B, no induction of lipid peroxidation was observed at 5 µg/mL for any NPs. A significant increase ($P<0.05$) in MDA levels was observed at all concentrations of uncoated and coated ZnO NPs. The bare ZnO NPs produced increasing lipid-peroxidation activity up to sixfold in comparison to controls with increased NP concentrations. Thin SiO_2/ZnO NPs caused less lipid peroxide production compared to bare ZnO NPs at all levels of NP concentrations. On the other hand, thick SiO_2/ZnO NPs at their maximum concentrations produced only twofold increases of lipid peroxide inductions in comparison to the other two NP groups.

Several studies have cited LPO and oxidative stress as important mechanisms in NP-induced cytotoxicity in various types of mammalian cells.[69–72] The NPs used in our study were also found to be capable of producing intracellular ROS with increased lipid peroxide levels. The LPO produced more free radicals, which could damage biomolecules, such as DNA, proteins, and lipids in combination with ROS. Therefore, LPO could also cause irrecoverable injury to the cell membrane, as indicated by an increased LDH release. The depletion of cell viability with NP exposure in combination with the increased level of LDH and LPO could be the primary mechanism for cytotoxicity in cells from dramatically increased oxidative stresses.[73] Previously, ZnO NPs induced oxidative stress in rat lung cells due to the liberation of zinc ion.[74] Due to the chemical and surface characteristics, the uncoated ZnO NPs could easily generate free radicals from interactions with cellular components. Our improved approach with SiO_2 coating on ZnO NPs could reduce potential damage to the cells by decreasing LDH leakage, oxidative stress, and lipid peroxide levels. However, additional studies will be necessary to investigate the potential endocytosis and cytotoxic mechanisms of SiO_2/ZnO NPs before and after UV irradiations with other different biological parameters for effective applications of ZnO NPs in toxicity-free material in cosmetic formulations.[75]

Conclusion

SiO_2-coated ZnO NPs were fabricated, and convincing evidence for their surface modification was obtained through HR-TEM, EDX, and zeta-potential analyses. Furthermore, the results indicated that the thick coating of SiO_2 effectively stabilized the ZnO NPs from light in comparison to bare and thin SiO_2/ZnO NPs. When the cytotoxicities of uncoated and coated ZnO NPs were compared, the thick SiO_2/ZnO NPs were less toxic, but minimal toxicity was still observed with HDFn cells. For thick SiO_2/ZnO NPs, the degree of LDH leakage, ROS production, and LPO release was less than that of the bare and thin SiO_2/ZnO NPs. Therefore, the cytotoxicity of the

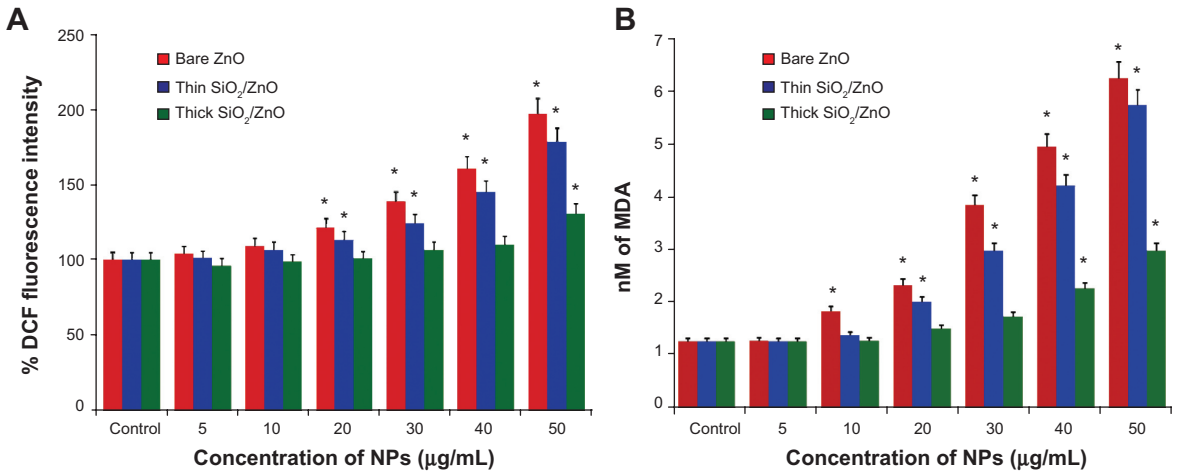

Figure 7 Intracellular oxygen and lipid peroxide measurements. (**A**) Levels of reactive oxygen species generation, and (**B**) lipid peroxide induction in HDFn cells after exposure to ZnO NPs for 48 hours.

Notes: *$P<0.05$. Values are means ± standard deviation of individual experiments performed in triplicate.

Abbreviations: HDFn, human dermal fibroblast neonatal; ZnO NPs, zinc oxide nanoparticles; thin SiO_2/ZnO, ZnO coated with a thin layer of SiO_2; thick SiO_2/ZnO, ZnO densely coated with SiO; DCF, dichlorofluorescein; MDA, malondialdehyde.

ZnO NPs decreased upon increased SiO_2 coating. Decreases in cytotoxicity arose presumably because of 1) fewer surface interactions of ZnO NPs with cells from the SiO_2 shell, 2) decreased release rate of zinc ion from ZnO NPs, and 3) a modified hydrophilic surface. In summary, a new approach for reduced toxicity with SiO_2 coating of ZnO NPs was devised and evaluated, resulting in decreased cytotoxicity.

Future examinations should focus on in vivo studies, assessing the effects of SiO_2/ZnO NPs on different organs and elucidating their toxicity effects. Additionally, it would be interesting to evaluate the applicability of toxicity-free SiO_2 ZnO NPs in cosmetic applications, such as skin creams.

Acknowledgment

This work was supported by the GRRC program of Gyeonggi Province (GRRC Gachon 2013-B04, Development of Microfluidic Chip for Diagnosing Diseases).

Disclosure

The authors report no conflicts of interest in this work.

References

1. Zhuang J, Liu M, Liu H. MAA-modified and luminescence properties of ZnO quantum dots. *Sci China Ser B Chem*. 2009;52(12):2125–2133.
2. Saad R, Thibutot S, Ampleman G, Hawari J. Sorptive removal of trinitroglycerin (TNG) from water using nanostructured silica-based materials. *J Environ Qual*. 2010;39(2):580–586.
3. Veerapandian M, Zhang L, Krishnamoorthy K, Yun K. Surface activation of graphene oxide nanosheets by ultraviolet irradiation for highly efficient anti-bacterials. *Nanotechnology*. 2013;24(39):395706.
4. Kleps I, Ignat T, Miu M, et al. Nanostructured silicon particles for medical applications. *J Nanosci Nanotechnol*. 2010;10(4):2694–2700.
5. Kim JE, Kim H, An SS, Maeng EH, Kim MK, Song YJ. In vitro cytotoxicity of SiO_2 or ZnO nanoparticles with different sizes and surface charges on U373MG human glioblastoma cells. *Int J Nanomedicine*. In press 2014.
6. Amarnath CA, Nanda SS, Papaefthymiou GC, Yi DK, Paik U. Nanohybridization of low-dimensional nanomaterials: synthesis, classification, and application. *Crit Rev Solid State Mater Sci*. 2013;38(1):1–56.
7. Tak Y, Hong SJ, Lee JS, Yong K. Fabrication of ZnO/CdS core/shell nanowire arrays for efficient solar energy conversion. *J Mater Chem*. 2009;19(33):5945–5951.
8. Kim C, Choi M, Jang J. Nitrogen-doped SiO_2/TiO_2 core/shell nanoparticles as highly efficient visible light photocatalyst. *Catal Commun*. 2010;11(5):378–382.
9. He Y, Lu HT, Sai LM, et al. Microwave-assisted growth and characterization of water-dispersed CdTe/CdS core-shell nanocrystals with high photoluminescence. *J Phys Chem B*. 2006;110(27):13370–13374.
10. Ramasamy M, Lee SS, Yi DK, Kim K. Magnetic, optical gold nanorods for recyclable photothermal ablation of bacteria. *J Mater Chem B*. 2014;2(8):981–988.
11. Li NF, Lei T, Ouyang C, He YH, Liu Y. An amperometric enzyme biosensor based on in situ electrosynthesized core-shell nanoparticles. *Synth Met*. 2009;159(15):1608–1611.
12. Yi DK, Sun IC, Ryu JH, et al. Matrix metalloproteinase sensitive gold nanorod for simultaneous bioimaging and photothermal therapy of cancer. *Bioconjug Chem*. 2010;21(12):2173–2177.
13. Yang P, Quan Z, Hou Z, et al. A magnetic, luminescent and mesoporous core-shell structured composite material as drug carrier. *Biomaterials*. 2009;30(27):4786–4795.
14. Subbiah R, Ramasundaram S, Du P, et al. Evaluation of cytotoxicity, biophysics and biomechanics of cells treated with functionalized hybrid nanomaterials. *J R Soc Interface*. 2013;10(88):20130694.
15. Kim YR, Lee EJ, Park SH, et al. Interactive survey of consumer awareness of nanotechnologies and nanoparticles in consumer products in South Korea. *Int J Nanomedicine*. In press 2014.
16. Wang ZL. Splendid one-dimensional nanostructures of zinc oxide: a new nanomaterial family for nanotechnology. *ACS Nano*. 2008;2(10):1987–1992.
17. Lee Y, Ruby DS, Peters DW, McKenzie BB, Hsu JP. ZnO nanostructures as efficient antireflection layers in solar cells. *Nano Lett*. 2008;8(5):1501–1505.
18. Yuranova T, Laub D, Kiwi J. Synthesis, activity and characterization of textiles showing self-cleaning activity under daylight irradiation. *Catal Today*. 2007;122(1):109–117.
19. Hanley C, Thurber A, Hanna C, Punnoose A, Zhang JH, Wingett DG. The influences of cell type and ZnO nanoparticle size on immune cell cytotoxicity and cytokine induction. *Nanoscale Res Lett*. 2009;4(12):1409–1420.
20. Serpone N, Dondi D, Albini A. Inorganic and organic UV filters: Their role and efficacy in sunscreens and suncare products. *Inorganica Chim Acta*. 2007;360(3):794–802.
21. Kim YR, Park SH, Lee JK, et al. Organization of research team for nano-associated safety assessment in effort to study nanotoxicology of zinc oxide and silica nanoparticles. *Int J Nanomedicine*. In press 2014.
22. Oberdörster G, Oberdörster E, Oberdörster J. Nanotoxicology: an emerging discipline evolving from studies of ultrafine particles. *Environ Health Perspect*. 2005;113(7):823–839.
23. Kim YR, Lee EJ, Park SH, et al. Comparative analysis of nanotechnology awareness in consumers and experts in South Korea. *Int J Nanomedicine*. In press 2014.
24. Brunner TJ, Wick P, Manse P, et al. In vitro cytotoxicity of oxide nanoparticles: comparison to asbestos, silica, and the effect of particle solubility. *Environ Sci Technol*. 2006;40(14):4374–4381.
25. Reddy K, Feris K, Bell J, Wingett DG, Hanley C, Punnoose A. Selective toxicity of zinc oxide nanoparticles to prokaryotic and eukaryotic systems. *Appl Phys Lett*. 2007;90(21):2139021–2139023.
26. Sharma V, Shukla RK, Saxena N, Parmar D, Das M, Dhawan A. DNA damaging potential of zinc oxide nanoparticles in human epidermal cells. *Toxicol Lett*. 2009;185(3):211–218.
27. Hu XK, Cook S, Wang P, Hwang HM. In vitro evaluation of cytotoxicity of engineered metal oxide nanoparticles. *Sci Total Environ*. 2009;407(8):3070–3072.
28. Zhu X, Zhu L, Duan Z, Qi R, Li Y, Lang Y. Comparative toxicity of several metal oxide nanoparticle aqueous suspensions to zebrafish (*Danio rerio*) early developmental stage. *J Environ Sci Health A Tox Hazard Subst Environ Eng*. 2008;43(3):278–284.
29. Wang B, Feng WY, Wang M. Acute toxicological impact of nano-and submicro-scaled zinc oxide powder on healthy adult mice. *J Nanopart Res*. 2008;10(2):263–276.
30. An SS, Kim YR, Park JI, Lee EJ, et al. Toxicity of 100 nm zinc oxide nanoparticles: a report of 90-day repeated oral administration in Sprague Dawley rats. *Int J Nanomedicine*. In press 2014.
31. Jia HY, Liu Y, Zhang XJ, et al. Potential oxidative stress of gold nanoparticles by induced-NO releasing in serum. *J Am Chem Soc*. 2008;131(1):40–41.
32. Arora S, Jain J, Rajwade J, Paknikar K. Cellular responses induced by silver nanoparticles: in vitro studies. *Toxicol Lett*. 2008;179(2):93–100.
33. Jang YJ, Simer C, Ohm T. Comparison of zinc oxide nanoparticles and its nano-crystalline particles on the photocatalytic degradation of methylene blue. *Mater Res Bull*. 2006;41(1):67–77.
34. Kango S, Kalia S, Celli A, Njuguna J, Habibi Y, Kumar R. Surface modification of inorganic nanoparticles for development of organic-inorganic nanocomposites – a review. *Prog Polym Sci*. 2013;38(8):1232–1261.
35. Hsiao IL, Huang YJ. Titanium oxide shell coatings decrease the cytotoxicity of ZnO nanoparticles. *Chem Res Toxicol*. 2011;24(3):303–313.

36. Yin H, Casey PS, McCall MJ, Fenech M. Effects of surface chemistry on cytotoxicity, genotoxicity, and the generation of reactive oxygen species induced by ZnO nanoparticles. *Langmuir*. 2010;26(19): 15399–15408.
37. Shim KH, Hulme J, Meang EH, Kim MK. Analysis of zinc oxide nanoparticles binding proteins in rat blood. *Int J Nanomedicine*. In press 2014.
38. Yi DK. A study of optothermal and cytotoxic properties of silica coated Au nanorods. *Mater Lett*. 2011;65(15):2319–2321.
39. Meyer K, Rajanahalli P, Ahamed M, Rowe JJ, Hong Y. ZnO nanoparticles induce apoptosis in human dermal fibroblasts via p53 and p38 pathways. *Toxicol In Vitro*. 2011;25(8):1721–1726.
40. Brinker CJ, Scherer GW. *Sol-Gel Science: The Physics and Chemistry of Sol-Gel Processing*. Waltham (MA): Academic; 1990.
41. Jaroenworaluck A, Sunsaneeyamatha W, Kosachan N, Stevens R. Characteristics of silica-coated TiO_2 and its UV absorption for sunscreen cosmetic applications. *Surf Interface Anal*. 2006;38(4):473–477.
42. Guo H, Qian H, Sun S. Hollow mesoporous silica nanoparticles for intracellular delivery of fluorescent dye. *Chem Cent J*. 2011;5(1):1.
43. Wroblewski F, Ladue JS. Lactic dehydrogenase activity in blood. *Proc Soc Exp Biol Med*. 1955;90(1):210–213.
44. Girotti AW. Lipid hydroperoxide generation, turnover, and effector action in biological systems. *J Lipid Res*. 1998;39(8):1529–1542.
45. Voelkel K, Krug HF, Diabate S. Formation of reactive oxygen species in rat epithelial cells upon stimulation with fly ash. *J Biosci*. 2003; 28(1):51–55.
46. Marnett LJ. Oxy radicals, lipid peroxidation and DNA damage. *Toxicology*. 2002;181–182:219–222.
47. Niedernhofer LJ, Daniels JS, Rouzer CA, Greene RE, Marnett LJ. Malondialdehyde, a product of lipid peroxidation, is mutagenic in human cells. *J Biol Chem*. 2003;278(33):31426–31433.
48. Alarifi S, Ali D, Alkahtani S, et al. Induction of oxidative stress, DNA damage, and apoptosis in a malignant human skin melanoma cell line after exposure to zinc oxide nanoparticles. *Int J Nanomedicine*. 2013;8: 983–993.
49. Oh WK, Kim S, Choi M, et al. Cellular uptake, cytotoxicity, and innate immune response of silica-titania hollow nanoparticles based on size and surface functionality. *ACS Nano*. 2010;4(9):5301–5313.
50. Baek M, Kim MK, Cho HJ, et al. Factors influencing the cytotoxicity of zinc oxide nanoparticles: particle size and surface charge. *J Phys Conf Ser*. 2011;304(1):012044.
51. An SS, Kim MK. Safety assessment of silica and zinc oxide nanoparticles. *Int J Nanomedicine*. In press 2014.
52. Torimoto T, Reyes JP, Iwasaki K, et al. Preparation of novel silica-cadmium sulfide composite nanoparticles having adjustable void space by size-selective photoetching. *J Am Chem Soc*. 2003;125(2):316–317.
53. Ramasamy M, Kim YJ, Gao H, Yi DK, An JH. Synthesis of silica coated zinc oxide-poly(ethylene-co-acrylic acid) matrix and its UV shielding evaluation. *Mater Res Bull*. 2014;51:85–91.
54. Zhai J, Tao X, Pu Y, Zeng XF, Chen JF. Core/shell structured ZnO/SiO_2 nanoparticles: preparation, characterization and photocatalytic property. *Appl Surf Sci*. 2010;257(2):393–397.
55. Palomares E, Clifford JN, Haque SA, Lutz T, Durrant JR. Control of charge recombination dynamics in dye sensitized solar cells by the use of conformally deposited metal oxide blocking layers. *J Am Chem Soc*. 2003;125(2):475–482.
56. Hong RY, Pan TT, Qian JZ, Li JZ. Synthesis and surface modification of ZnO nanoparticles. *Chem Eng J*. 2006;119(2–3):71–81.
57. Chavanpatil MD, Khdair A, Panyam J. Nanoparticles for cellular drug delivery: mechanisms and factors influencing delivery. *J Nanosci Nanotechnol*. 2006;6(9–10):9–10.
58. Unfried K, Albrecht C, Klotz LO, Von Mikecz A, Grether-Beck S, Schins RP. Cellular responses to nanoparticles: target structures and mechanisms. *Nanotoxicology*. 2007;1(1):52–71.
59. Shim KW, Jeong KH, Bae SO, et al. Assessment of ZnO and SiO_2 nanoparticle permeability through and toxicity to the blood–brain barrier using Evans blue and TEM. *Int J Nanomedicine*. In press 2014.
60. Barnes CA, Elsaesser A, Arkusz J, et al. Reproducible comet assay of amorphous silica nanoparticles detects no genotoxicity. *Nano Lett*. 2008;8(9):3069–3074.
61. Jeng HA, Swanson J. Toxicity of metal oxide nanoparticles in mammalian cell. *J Environ Sci Health*. 2006;41(12):2699–2711.
62. Lison D, Thomassen LC, Rabolli V, et al. Nominal and effective dosimetry of silica nanoparticles in cytotoxicity assays. *Toxicol Sci*. 2008;104(1):155–162.
63. Waters KM, Masiello LM, Zangar RC, et al. Macrophage responses to silica nanoparticles are highly conserved across particle sizes. *Toxicol Sci*. 2009;107(2):553–569.
64. Shim KH, Hulme J, Maeng EH, Kim MK, An SS. Analysis of SiO_2 nanoparticles binding proteins in rat blood and brain homogenate. *Int J Nanomedicine*. In press 2014.
65. Mallick S, Sun IC, Kim K, Yi DK. Silica coated gold nanorods for imaging and photo-thermal therapy of cancer cells. *J Nanosci Nanotechnol*. 2013;13(5):3223–3229.
66. Moos PJ, Chung K, Woessner D, Honeggar M, Cutler NS, Veranth JM. ZnO particulate matter requires cell contact for toxicity in human colon cancer cells. *Chem Res Toxicol*. 2010;23(4):733–739.
67. Buerki-Thurnherr T, Xiao L, Diener L, et al. In vitro mechanistic study towards a better understanding of ZnO nanoparticle toxicity. *Nanotoxicology*. 2013;7(4):402–416.
68. Deng X, Luan Q, Chen W, et al. Nanosized zinc oxide particles induce neural stem cell apoptosis. *Nanotechnology*. 2009;20(11):115101.
69. Nel A, Xia T, Madler L, Li N. Toxic potential of materials at the nanolevel. *Science*. 2006;311(5761):622–627.
70. An SS, Kim YR, Lee SY, Lee EJ, et al. Toxicity of colloidal silica nanoparticles administered orally for 90 days in rats. *Int J Nanomedicine*. In press 2014.
71. Hanley C, Layne J, Punnoose A, et al. Preferential killing of cancer cells and activated human T cells using ZnO nanoparticles. *Nanotechnology*. 2008;19(29):295103.
72. Singh S, Shi TM, Duffin R, et al. Endocytosis, oxidative stress and IL-8 expression in human lung epithelial cells upon treatment with fine and ultrafine TiO_2: role of the specific surface area and of surface methylation of the particles. *Toxicol Appl Pharmacol*. 2007;222(2): 141–151.
73. Ott M, Gogvadze V, Orrenius S, Zhivotovsky B. Mitochondria, oxidative stress and cell death. *Apoptosis*. 2007;12(5):913–922.
74. Fukui H, Horie M, Endoh S. Association of zinc ion release and oxidative stress induced by intratracheal instillation of ZnO nanoparticles to rat lung. *Chem Biol Interact*. 2012;198(1):29–37.
75. DeLouise LA. Applications of nanotechnology in dermatology. *J Invest Dermatol*. 2012;132(3 Pt 2):964–975.